LA-UR-00- - 3792

TITLE: BEAM HALO IN PROTON LINAC BEAMS

AUTHOR(S): Thomas P. Wangler LANSCE-1
Kenneth R. Crandall TECHSOURCE

SUBMITTED TO: LINAC 2000 Conference
Monterey, California
August 21-25, 2000

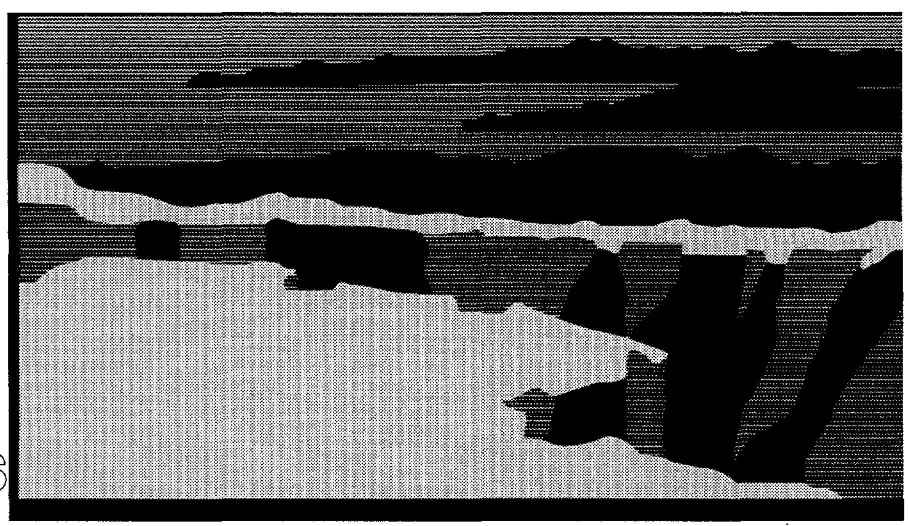

Los Alamos
NATIONAL LABORATORY

DISCLAIMER

BEAM HALO IN PROTON LINAC BEAMS

T.P.Wangler, Los Alamos National Laboratory, Los Alamos, NM 87545
K.R.Crandall, TechSource, Santa Fe, NM 87594-1057

Abstract

In this paper we review the present picture of beam halo in proton linacs. Space-charge forces acting in mismatched beams have been identified as a major cause of beam-halo. We present a definition of halo based on a ratio of moments of the distribution of the beam coordinates. We find from our initial studies that for halo defined in this way, a beam can have rms emittance growth without halo growth, but halo growth is always accompanied by rms emittance growth. We describe the beam-halo experiment that is in preparation at Los Alamos, which will address questions about the beam profiles, maximum particle amplitudes, and rms emittance growth associated with the halo.

1 INTRODUCTION

The existence of beam halo is an undesirable characteristic of high-intensity beams. Under certain conditions in proton beams some particles can acquire enough energy from the repulsive space-charge forces within the beam to form a halo at the periphery. The formation of halo is an important issue, because if the halo particles are lost at high energies (above about 100 MeV) on the walls of the beamline structures, they will induce unwanted radioactivity, which can limit the operating beam current. The next generation of proton-linac applications, including projects to produce tritium[1], and to transmute radioactive wastes[2], require beams with average currents that are higher than for the present LANSCE linac (1 mA) by factors of 20 to 100. These higher average beam currents will increase the risk of beam losses unless the formation of beam-halo can be suppressed. Consequently, it has become even more important to ensure that the physical causes of the halo are understood.

2 PRACTICAL HALO DEFINITION AND SOME GENERAL OBSERVATIONS

One may wonder why beams develop halo. An explanation lies in the statement that halo formation is fundamentally a consequence of classical filamentation in 6D phase space from nonlinear forces. The 6D phase-space filaments project as an extended diffuse halo in 2D phase spaces [3] where they are observed. Nevertheless, an issue that has contributed to some confusion has been the lack of a definition of the halo. We will present a definition of halo in coordinate space which we have found to be useful. First, we define a new quantity that we will call the beam-profile parameter. For a continuous beam the definition of the beam-profile parameter in x-coordinate space will be

$$h_x = \langle x^4 \rangle^{1/4} / \langle x^2 \rangle^{1/2} - 2^{1/4},$$

and a similar definition can be made of h_y, a beam-halo parameter for the y coordinate, by replacing y for x. For an ellipsoidal bunch the definition in x-coordinate space is

$$h_x = \langle x^4 \rangle^{1/4} / \langle x^2 \rangle^{1/2} - (15/7)^{1/4},$$

and likewise for h_y and h_z in the other two planes. These are dimensionless quantities, which are independent of the beam intensity, easily calculated from moments of the particle distribution, dependent only on the profile shape, zero for a uniform density beam, and for non-hollow beams, increasing with increasing nonuniformity. As halo develops in the beam, increasing the population of large amplitude particles, the beam profile parameter increases. The beam-profile parameter has been evaluated for some of the familiar distributions, as shown in Table 1.

Table 1. Some beam profile parameter values

Spatial Distribution	Beam-profile parameter h
Uniform ellipse (K-V)	0.0
Parabolic (4D Waterbag)	$(3/2)^{1/2}-2^{1/4}= 0.03554$
Gaussian ellipse	$3^{1/4}-2^{1/4}= 0.1269$
Uniform ellipsoid	0.0
Parabolic ellipsoid	$(7/3)^{1/4}-(15/7)^{1/4}=0.02603$
Gaussian ellipsoid	$3^{1/4}-(15/7)^{1/4}=0.1062$

We have adopted a somewhat arbitrary but practical criterion that a beam will be said to contain halo in coordinate space when its beam-profile parameter exceeds the parameter value for a Gaussian beam. By this criterion equilibrium beams and rms-matched beams generally have no halo. Beams with tails that exceed those of a Gaussian beam are said to have halo. Rms mismatched beams typically have halo.

Given the halo criterion based on the beam profile parameter, we can now answer several interesting physics questions. Under what conditions is beam halo observed, and is there a relationship between beam halo and emittance growth? Using computer simulations we have examined several common situations and have reached the following preliminary conclusions. No halo is formed in equilibrium beams or rms-matched beams that have no initial halo. Likewise, beams with no initial halo that expand in free space do not form halo during the expansion. However, rms-matched beams and expanding beams can have emittance growth during charge redistribution as field energy is converted to thermal energy, the beam-profile parameter decreases, and the beam tends to become more spatially uniform.[4] Therefore, it is possible to have emittance growth without an increase in the beam profile parameter and without forming halo. Rms-mismatched beams that have no initial halo do form halo, always accompanied by emittance growth. The emittance growth appears to be correlated with the increases in the maximum of the oscillating beam-profile parameter. Thus, emittance can grow without halo growth, but halo growth always leads to emittance growth.

Our definition of halo in coordinate space does not provide all answers for a full description of the halo. For example, an important quantity of practical interest that is not obtained from the moments of the distribution is the maximum amplitude of the halo particles. From the beam profile parameter, we are not able to answer the question How far out does the halo extend? Furthermore, in a mismatched beam the beam-profile parameter oscillates at the mismatch frequency as the outer filaments rotate in phase space. The halo can temporarily populate the momentum-space projection, where it can't be observed in the coordinate projections. The maximum value of the oscillating beam-profile parameter oscillations should be used as a measure of the halo that exists in phase space.

3 BEAM HALO IN PROTON LINACS

Multiparticle simulation studies of round beams in uniform linear focusing channels have provided some useful physical insights into the dynamics of high-current beams. For a nonequilibrium beam injected with the correctly matched rms size, the initial radial distribution relaxes with accompanying emittance growth over a time of only about one quarter plasma period to a quasi-equilibrium state with an approximately uniform central core in real space and with an edge that falls off over a distance approximately equal to the Debye length [4]. The relative sizes of the central core and the Debye edge depend on whether the beam is emittance or space-charge dominated. In the extreme space-charge limit the size of the Debye edge approaches zero and the spatial density of the core is uniform, whereas in the emittance-dominated limit the profile is dominated by the Debye edge and the spatial density of the beam is approximately Gaussian [5]. Beam-dynamics simulations show that halo is not a significant characteristic in rms-matched beams.

In numerical simulation studies of rms mismatched beams in both uniform and periodic channels, halo was observed in the particle distributions that was much more extended and more densely populated [6-10] than the small Debye tail of a matched beam. The simulation results suggested a simple particle-core model to describe the motion of halo particles in a mismatched beam. In the model a central charge distribution or core oscillates as a consequence of the initial mismatch, and particles, including those in the initial Debye edge, are represented by individual test particles that interact with the external focusing force and with the time-dependent space-charge field of the core [11,12]. Various aspects of a particle core model have been studied at several laboratories [13-24]. Perhaps the most significant result obtained from an approximate analytic solution of the model equations [12] has been the discovery that the interaction between the particles and the oscillating core is described by a parametric resonance that is effective in driving some particles to large amplitudes. The resonance affects particles whose oscillation frequencies are about one half the frequency of the oscillating core. This simple model is sufficient to describe the maximum amplitudes that are observed in the beam-dynamics simulations in uniform focusing channels.

In a typical proton linac, bunches are formed which have an approximately spheroidal shape in the beam frame with a range of aspect ratios that may include very long bunches and nearly spherical bunches. To model the transverse dynamics of halo particles in mismatched beams where the bunch length is several times larger than the radius, it is convenient to use the simple particle-core model based on transverse particle motion in the space-charge field of a continuous oscillating cylindrical beam core. The core is assumed to be mismatched symmetrically to excite a breathing mode where the x and y excursions are equal and in phase. To model the halo-particle dynamics of a spherical bunch one can use a particle-core model with a spherical core, and a breathing mode excitation where the x, y, and z excursions are all in phase. In either case the space-charge field of the beam is approximated by replacing the unknown beam distribution with that of an equivalent-uniform beam core, where the equivalent beam has the same rms size as the actual beam. We have found that the particle-core model results are not sensitive to whether the core-density distribution is uniform or Gaussian.

Several interesting aspects of the particle-core model should be mentioned. One question concerns the origin of the halo particles. For realistic particle distributions in accelerators with linear focusing forces, excluding the singular K-V distribution and excluding the extreme space-charge limit, a Debye tail exists at the beam edge that will usually extend into the region of influence of the parametric resonance. For these beams, K-V core instabilities are not required to explain the existence of particles near the core that can be resonantly excited, although if such instabilities are present [18,19,21] they could feed additional particles into the tail. Thus, the particle-core model can represent a beam whose initial density distribution includes particles that populate a finite-size Debye tail, and the fraction of those particles that are included within the region of influence of the resonance determines a minimum population of the halo. Next, a very important feature of the particle-core model is that it predicts the maximum amplitude for the resonantly driven particles as a function of the strength of the mismatch. From numerical simulations in uniform focusing channels good agreement is obtained for this maximum amplitude for a variety of particle distribution, which provides strong supporting evidence for the model[25]. Finally, we find that the maximum amplitude for any mismatch strength is proportional to the matched rms beam size. Using the analytic solution relating the matched rms size of the beam core to the current, emittance, and focusing strength, we have obtained a scaling formula for the size of the transverse beam halo[25]. The formula predicts that for a given mismatch strength the maximum transverse halo amplitude increases with increasing beam current, and with decreasing frequency, bunch length, and focusing strength. Estimates of the growth time of the halo have been made from the model. Generally, these estimated growth times are not very sensitive to the mismatch strength, but increase strongly with tune depression ratio as the beam becomes more emittance dominated. Comparisons of these growth times from the model with numerical simulations show that the results in Fig.7 are approximately correct to within about a factor of 2. However, the halo growth times from the simulations depend on the initial particle distribution, and are often difficult to define in an unambiguous way. As the beam becomes more space-charge dominated, chaotic motion is observed. The main effect of the chaos is not so much to increase the maximum halo amplitude, but to increase the population of the halo.

The simple spherical model is a first approximation for a bunched beam with nearly equal semiaxes excited in a breathing mode. But the spherical model neglects several effects, two other core oscillation modes (quadrupole mode and antisymmetric mode), effects associated with aspect ratios different then unity, and nonlinear longitudinal external fields. The study of a more general spheroidal bunch model [26] shows that the halo physics does depends on the bunch aspect ratio. For long bunches (approximately z > 2r) the transverse and longitudinal envelope and halo dynamics are weakly coupled. The symmetric or breathing mode is dominated by transverse motion and generates transverse halo. The antisymmetric mode where the z core excursions are out of phase with the x and y excursions is dominated by longitudinal motion and generates longitudinal halo. For nearly spherical bunches the transverse and longitudinal envelope and halo dynamics are strongly coupled.

Nonlinear rf focusing can be added to the particle-core model to represent the nonlinear rf effects in the longitudinal dynamics. As the particle amplitude increases, a defocusing rf nonlinear longitudinal force term can add significantly to the main linear term (which is focusing if the bunch arrives at the rising part of the rf waveform) to impede the increase in the net focusing force and disrupt the parametric resonance condition [22]. This change has a significant effect on the longitudinal dynamics of the particles by reducing the particle frequencies and amplitudes. Simulations confirm that the longitudinal halo is well confined within the rf bucket except for extreme values of the mismatch. Beam loss from longitudinal halo may be less of a concern in a linac than the transverse halo.

We believe that the beam mismatch acts in two ways to produce the halo. First, even without space-charge forces, a mismatch produces coherent oscillations of all the beam particles and an immediate increase in particle transverse excursions. Second, the nonlinear space-charge force, acting while the beam particles are oscillating through the beam, slowly drives some particles to even larger amplitudes through parametric resonance with the coherent beam oscillations. In determining the expected beam mismatch for a high-current linac design, one must account for the fact that in a real linac the beam may be mismatched as a result of a large number of small errors distributed along the linac, rather than from a single mismatch, as is described by the particle-core model. A realistic prediction of the mismatch and the halo amplitudes for a given linac should be made from multiparticle simulation studies including random errors based on realistic expectations [27]. Finally, most of the simulation work to study beam halo has been for uniform focusing channels. We believe that more work should to be done to study halo in periodic channels.

4 BEAM HALO EXPERIMENT

We have designed and are installing a beamline at the end of the Low-Energy Demonstration Accelerator (LEDA) [28] to carry out a first experimental study of beam-halo formation in a proton beam (see Fig.1). The LEDA facility will deliver a 6.7-MeV, 100-mA proton beam from the 350-MHz radio-frequency quadrupole (RFQ) [29] to the new beamline. The beamline will consist of a periodic array of 52 quadrupole magnetic lenses for transverse confinement of the beam, and beam-diagnostic devices to monitor and measure the beam properties. To study the beam halo we will set the quadrupole strengths to deliberately establish mismatch conditions favorable for halo formation, and measure and analyze the beam profiles. The measured halo effects will be compared with those predicted by our beam-dynamics simulation codes, and the comparisons will enable us either to confirm that the computer models are correct or identify possible missing physics effects that may need to be incorporated.

The beamline parameters can be varied to establish different known mismatch conditions that are more or less favorable for formation of halo. We are interested in determining the maximum amplitudes of the beam particles, and the particle distributions and the corresponding beam-profile parameters. We are also interested in the rms emittances of the beam, which can be determined experimentally from multiple measurements of the rms beam sizes from the beam profiles at different locations. Another experimental objective is to explore those regions beyond where halo is predicted by simulations to ensure that there are no other important sources of halo than those predicted by the simulation codes.

The detailed theoretical predictions of the beam halo are made using beam-dynamics simulation codes, which use multiparticle simulation methods to follow the evolution of the beam particles, including the quadrupole focusing forces and the repulsive space-charge forces that act on all the particles. The simulation codes all contain certain approximations, and different computer codes are used to provide internal checks. The experiment uses the output beam from the LEDA RFQ. The RFQ is capable of delivering a continuous beam, which leaves the RFQ as a sequence of subnanosecond bunches at a 350-MHz rate. To avoid beam destruction of the thin wires used for measurement of the beam profiles, the beam will be pulsed at about a 1- to 2-Hz rate with short 20- to 30-microsecond long macropulses. The beam-transport line will be installed immediately behind the LEDA RFQ. The lattice is spatially periodic containing a sequence of alternating focusing and defocusing quadrupole magnets with a 21-cm cell length for each of the 52 cells. This results in 26 focusing periods, and the total length of the beamline is about 10.9m. The beam-pipe diameter is limited by the steel polepieces in the quadrupole magnets; the inner beam-pipe radius is about 1.4 cm. As the beam propagates in the beamline, the bunches expand and eventually after a few meters each bunch overlaps with adjacent bunches forming an approximately continuous beam. The main effect of the unavoidable debunching on the transverse halo is to reduce the effective beam current and accompanying space-charge forces that affect the transverse halo formation. However, the magnitude of the halo for a mismatched beam is still predicted to be large and easily measurable.

Initially, the strengths of the 52 quadrupole magnets will be set to provide a matched condition for the beam. The strengths of the first four quadrupole magnets will be varied to either match the beam or create deliberate mismatches that excite beam oscillations and halo. The mismatch-induced beam oscillations in a continuous beam consist of two kinds, a breathing mode, where the oscillations in the two transverse planes x and y are in phase, or a quadrupole mode, where the oscillations are out of phase.

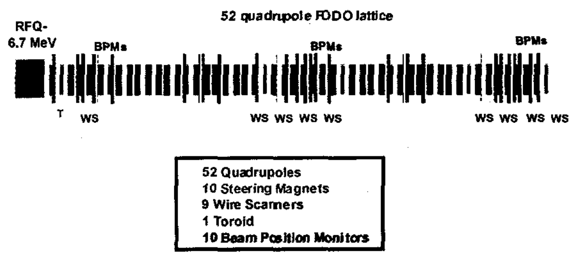

Fig.1. Fully instrumented beam halo experiment

The transverse beam profiles will be measured using an array of specially constructed beam-profile scanners. The nominal locations of the scanners are near the middle of the drift space between a pair of quadrupoles. The beam-profile scanner is the most important diagnostic device for the experiment. Each scanner contains of a single 33-micron diameter graphite wire for measurements of the high-intensity central beam core in each transverse plane. In addition each scanner contains a pair of copper plates, one on each side of each wire to intercept and measure the beam intensity in the low-density halo region. The wire will provide intensity measurements over a dynamic range of about 1000. The plates will extend the lower limit of this range by another factor of 10 to 100 for the halo measurements. For a beam with a Gaussian profile, the wire provides a transverse profile measurement out to about 4 standard deviations, and the plate extends this to about 5 standard deviations.

5 BEAM DYNAMICS SIMULATION STUDIES

In Figs. 3 through 10 we will show some beam-dynamics simulation results for the matched beam, and a breathing-mode mismatched beam using 10,000 particles per simulation run and using the SCHEFF space-charge subroutine. The input-particle distribution for the simulations was obtained from a previous beam-dynamics simulation through the LEDA RFQ.

Fig. 3 shows approximately constant values at the center of the 52 drift spaces along the beamline for the root-mean-square beam sizes in both transverse planes, indicating that the beam is approximately matched. Fig.4 shows the result of a mismatch caused by the adjustment of the first four quadrupole strengths. Fig. 4 shows in-phase oscillations for x_{rms} and y_{rms} indicating that the breathing-mode has been excited.

Comparison of Figs. 3 and 4 shows a large factor of about 2 increase in the maximum particle amplitude when the beam is mismatched. Fig. 5 shows the beam-profile parameters for the x and y planes versus distance along the beamline for the matched beam. The values for uniform, parabolic, and Gaussian beams are shown for reference. The lack of parameter excursions above the Gaussian level in Fig.5 indicates an absence of halo. Fig.

6 shows the beam-profile parameters versus distance along the beamline for the mismatched beam. The excursions above the Gaussian level in Fig.6 indicate the presence of beam halo in both planes. Figs. 7 and 8 show the beam cross sections at the center of drift space after quadrupole 49 for the matched and mismatched cases, respectfully, showing an absence of halo for the matched beam and the presence of halo for the mismatched beam. Figs. 9 and 10 show the projections of the beam cross sections of Figs. 7 and 8 onto the horizontal axis, again showing an absence of halo for the matched beam and the presence of halo for the mismatched beam.

Simulations with 100M particles, using the IMPACT code on a fast parallel computer, have also been carried out. These simulations agree very well with the results shown in the figures. The maximum amplitudes from IMPACT for the breathing-mode mismatch are larger than that of the SCHEFF runs by only about 10%. Rms emittances and beam-profile parameters agree to within about 10%.

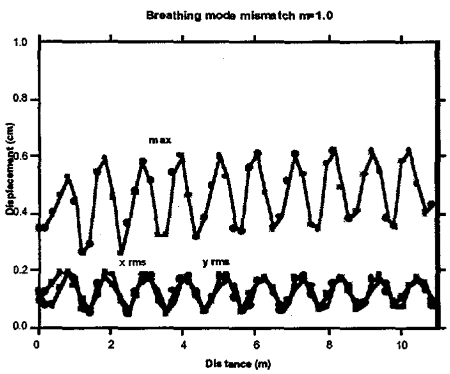

Fig. 4. Rms beam sizes and maximum particle displacements at 52 drift-space locations versus distance along beamline for the mismatched beam as predicted by a computer simulation. The in-phase oscillations for x_{rms} in red and y_{rms} in blue indicate that the symmetric or breathing-mode has been excited.

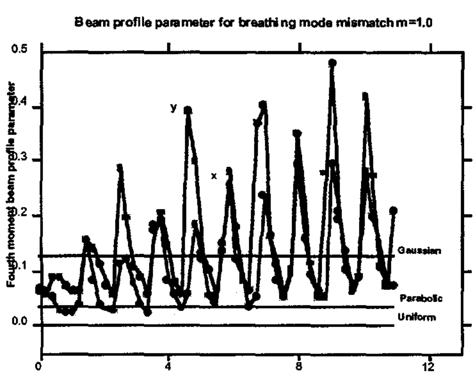

Fig. 6. Beam-profile parameter versus distance along beamline for the symmetrically mismatched beam as predicted by a computer simulation. The values for uniform, parabolic, and Gaussian beams are shown for reference. The excursions above the Gaussian level indicate the presence of beam halo in both the x and y planes.

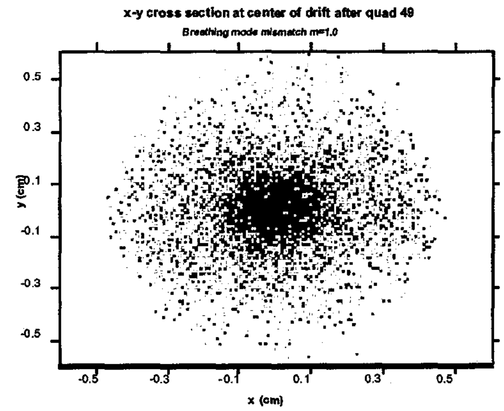

Fig. 8. Beam cross section showing the presence of halo at center of drift after the quadrupole 49 for the symmetrically mismatched beam as predicted by a computer simulation.

SUMMARY

In this paper we have reviewed the present picture of beam halo in linacs. We have presented a simple definition of halo based on a ratio of moments of the distribution of the beam coordinates relative to a Gaussian reference distribution. We find from our initial studies that for halo defined in this way, a beam can have rms emittance growth without halo growth, but halo growth is always accompanied by rms emittance growth.

We have reviewed the present picture of beam halo growth in proton linacs, and we believe that although a lot is known about halo in uniform focusing channels, more need to be done to study beam halo growth in periodic focusing channels. We have described the beam-halo experiment at the LEDA facility at Los Alamos, which will provide the first experimental tests of our understanding of halo formation in high-current proton beams. The 52-quadrupole beamline and the beam diagnostics are being built, tested, and installed. Experimental measurements are expected to take place from October through the end of January, 2001.

ACKNOWLEDGMENTS

The authors acknowledge support from the U.S. Department of Energy, and thank R.Ryne, Ji Qiang, R.L.Gluckstern, D. Gilpatrick, and C. Allen for helpful discussions.

REFERENCES

[1] P.W.Lisowski, "The Accelerator Production of Tritium Project," Proc. 1997 Particle Accelerator Conf., Vancouver, British Columbia, Canada, (IEEE, Catalog No.97CB36167, 1997) 3780-3784.

[2] "A Roadmap for Developing Accelerator Transmutation of Waste (ATW) Technology," A Report to Congress, DOE/RW-0519, October 1999.

[3] T. P. Wangler, *Computational Accelerator Physics Conference* (CAP93), 1993, AIP Conf. Proc. **297**, edited by Robert Ryne, (AIP Press, New York, 1993), p 9.

[4] T. P. Wangler, K. R. Crandall, R. S. Mills, and M. Reiser, IEEE Trans. Nucl. Sci. **32**, 2196 (1985).

[5] J. D. Lawson, *The Physics of Charged Particle Beams* (Clarendon Press, Oxford, 1988), Matched Beam in a Uniform Focusing Field, 1st edition, pp. 211-213.

[6] J. Struckmeier and M. Reiser, Part. Accel. **14**, 227 (1984).

[7] A. Cucchetti, M. Reiser, and T. P. Wangler, *Proceedings of the IEEE 1991 Particle Accelerator Conference,* 1991, IEEE Catalog No. 91CH3038-7, edited by L. Lizama and J. Chew, (IEEE, New York, 1991), p. 251.

[8] M. Reiser, *Proceedings of the IEEE 1991 Particle Accelerator Conference,* 1991, IEEE Catalog No. 91CH3038-7, edited by L. Lizama and J. Chew, (IEEE, New York, 1991), p. 2497.

[9] T. P. Wangler, *Computational Accelerator Physics Conference* (CAP93), 1993, AIP Conf. Proc. **297**, edited by Robert Ryne, (AIP Press, New York, 1993), p 9.

[10] O. A. Anderson and L. Soroka, 1987 Particle Accelerator Conference, 1987, IEEE Catalog No. 87CH2387-9, edited by E.R. Lindstrom and L. S. Taylor, (IEEE, New York, 1987), p.1043.

[11] J.S. O'Connell, T.P. Wangler, R.S. Mills, and K.R. Crandall, *Proceedings of the 1993 Particle Accelerator Conference,* 1991, IEEE Catalog No. 93CH3279-7, edited by S. T. Corneliussen, (IEEE, New York, 1991), p. 3657.

[12] R. Gluckstern, Phys. Rev. Lett. **73**, 1247 (1994).

[13] J. Lagniel, Nucl. Inst. Meth. A**345**, 46 (1994).

[14] J. Lagniel, Nucl. Inst. Meth., A**345**, 405 (1994).

[15] T. P. Wangler, Los Alamos Report LA-UR-94-1135 (1994).

[16] R. Jameson, Los Alamos Report LA-UR-93-1209 (1994).

[17] R. Ryne, S. Habib, and T.P. Wangler, AIP Conf. Proc., **346**, 383 (1994).

[18] R. L. Gluckstern, W. H. Cheng, and H. Ye, Phys. Rev. Lett. **75**, 2835 (1995).

[19] Robert L. Gluckstern, Wen-Hao Cheng, Sergey S. Kurennoy, and Huanchan Ye, Phys. Rev. E **54**, 6788 (1996).

[20] T. P. Wangler, R. W. Garnett, E. R. Gray, R. D. Ryne, and T. S. Wang, *Proceedings of XVIII International Linear Accelerator Conference*, Geneva, Switzerland, 1996, CERN report CERN 96-07, edited by C. Hill and M. Vretenar, (CERN, Geneva, 1996) p. 372.

[21] Robert L. Gluckstern and Sergey S. Kurennoy, *1997 Particle Accelerator Conf.*, Vancouver, British Columbia, Canada, p. 1950.

[22] J. Barnard and S. Lund, *1997 Particle Accelerator Conf.*, Vancouver, British Columbia, Canada, p. 1929 and p.1932.

[23] T. P. Wangler, E. R. Gray, S. Nath, and K. R. Crandall, *1997 Particle Accelerator Conf.*, Vancouver, British Columbia, Canada, p. 915.

[24] H. Okamoto and M. Ikegami, Phys. Rev. E. **55**, 4694 (1997).

[25] Thomas P. Wangler, "Beam Halo Formation in High Intensity Proton Beams", Proc. 2nd ICFA Advanced Accelerator Workshop on the Physics of High Brightness Beams, November 9-12, 1999, UCLA, Los Angeles, CA.

[26] R. L. Gluckstern, A. V. Fedotov, S. S. Kurrenoy, and R. D. Ryne, Phys. Rev. E. **58**, 4977 (1998).

[27] Thomas P. Wangler, "APT Linac Design for Low Beam Loss", 7th ICFA Mini-Workshop on High Intensity High Brightness Beams - Beam Halo and Scraping, Lake Como, WI, September 13-15, 1999.

[28] J.D.Schneider,"Operation of the Low-Energy Demonstration Accelerator: The Proton Injector for APT," Proc. 1999 IEEE Particle Accelerator Conference (IEEE, Catalog No. 99CH36366, 1999), 503-507.

[29] D. Schage et al., "CW RFQ Fabrication and Engineering," Proc. XIX International Linac Conference (Argonne National Laboratory, ANL-98/28, 1998), 679-683.